Calculation of TAE mode structure in general axisymmetric toroidal geometry[1]

Guangyu Wei[1,2], Matteo Valerio Falessi[2], Tao Wang[1,2], Fulvio Zonca[2,1], Zhiyong Qiu[3,2]

1 Institute for Fusion Theory and Simulation, School of Physics, Zhejiang University, Hangzhou, China
2 Center for Nonlinear Plasma Science and C.R. ENEA Frascati, Via E. Fermi 45, Frascati, Italy
3 Key Laboratory of Frontier Physics in Controlled Nuclear Fusion and Institute of Plasma Physics, Chinese Academy of Sciences, Hefei, China

[1] G. Wei, M. V. Falessi, T. Wang, F. Zonca, and Z. Qiu. Physics of Plasmas 31, 072505 (2024).

Outline

- **Background**
- **Theoretical framework**
  - Model equations: ideal MHD equations in ballooning space
  - Solving method: Floquet solutions $\Longrightarrow$ boundary condition
- **Numerical results**
  - Frequency and mode structure of TAE in DTT (slow sound approximation)
  - Effect of triangularity on TAE (slow sound approximation)
  - Finite damping rate and radial singular structure of TAE due to the coupling with acoustic continuum (full SAW-ISW system)
- **Summary and prospect**

Outline

- **Background**
- **Theoretical framework**
  - Model equations: ideal MHD equations in ballooning space
  - Solving method: Floquet solutions $\Longrightarrow$ boundary condition
- **Numerical results**
  - Frequency and mode structure of TAE in DTT (slow sound approximation)
  - Effect of triangularity on TAE (slow sound approximation)
  - Finite damping rate and radial singular structure of TAE due to the coupling with acoustic continuum (full SAW-ISW system)
- **Summary and prospect**

Background

Continuous spectrum and Alfvén eigenmodes (AEs)

Continuous spectrum in DTT device using FALCON [Falessi PoP 19, Falessi JPP 20]

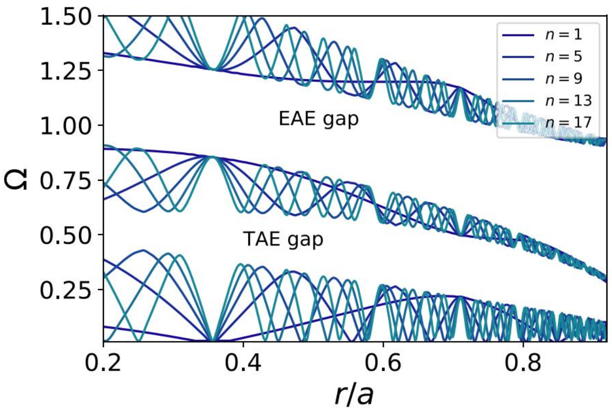

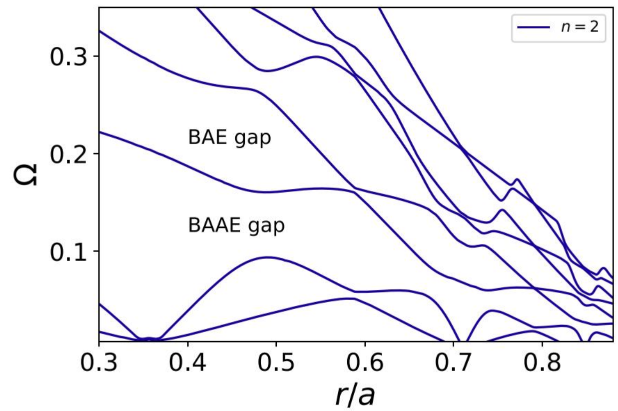

Convective and diffusive EP losses induced by TAE in ASDEX Upgrade [García-Munõz PRL 10]

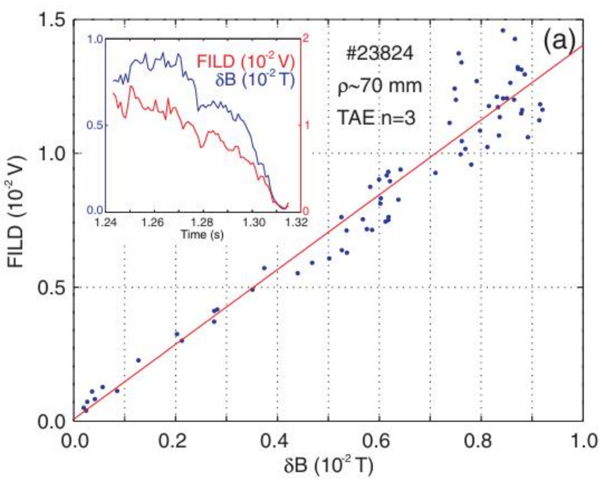

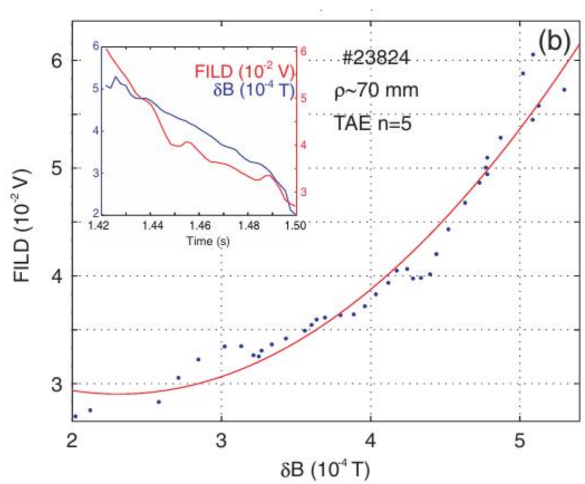

Calculation of frequency and mode structure of AE is important!

Background

Effect of negative triangularity (NT)

Strong reduction of electron heat flux in NT was first observed in TCV [Camenen NF 07]

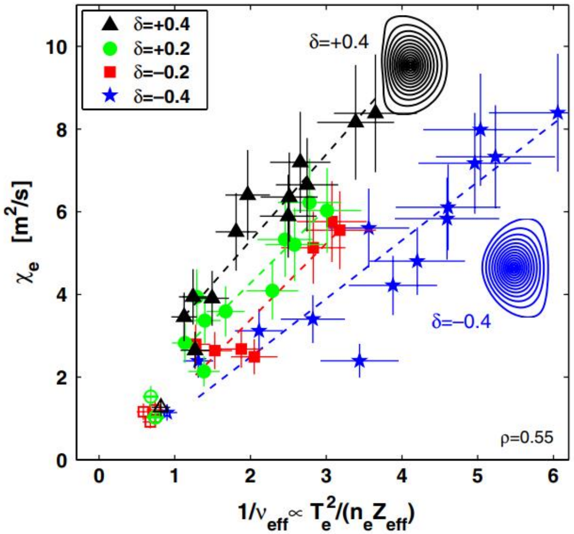

DIII-D team showed the H-mode-like confinement in NT L-mode, natural ELM-free [Austin PRL 19]

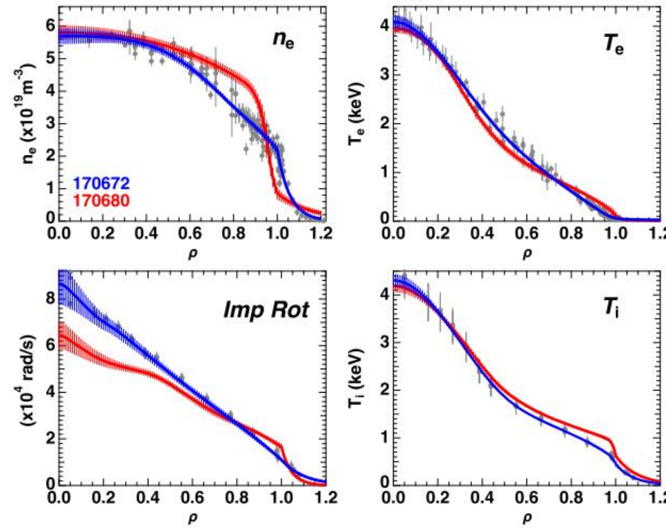

Red: PT
Blue: NT

MEGA simulation shows that TAEs have lower energy and growth rate in NT [Oyola IAEA 23]

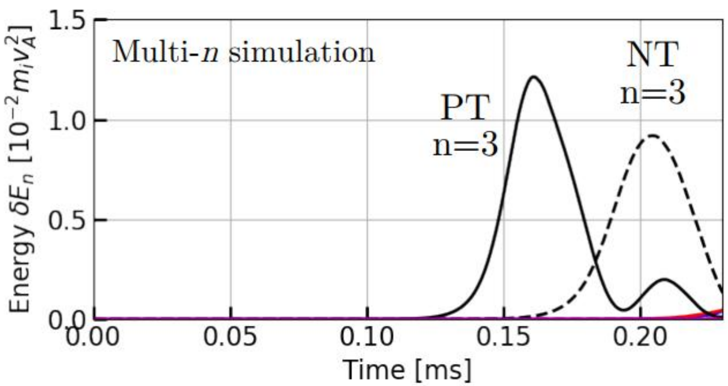

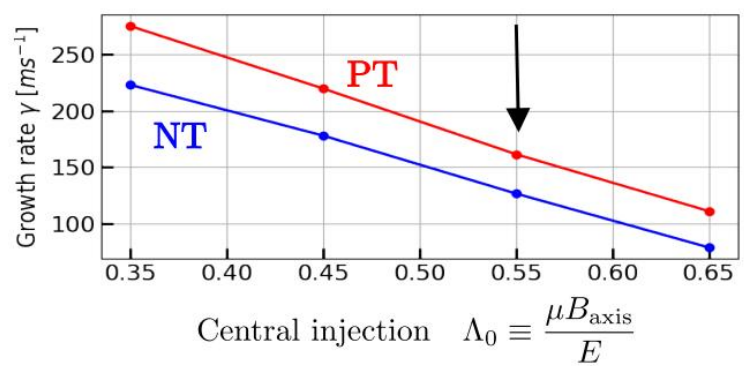

Outline

- **Background**
- **Theoretical framework**
  - Model equations: ideal MHD equations in ballooning space
  - Solving method: Floquet solutions $\Longrightarrow$ boundary condition
- **Numerical results**
  - Frequency and mode structure of TAE in DTT (slow sound approximation)
  - Effect of triangularity on TAE (slow sound approximation)
  - Finite damping rate and radial singular structure of TAE due to the coupling with acoustic continuum (full SAW-ISW system)
- **Summary and prospect**

Model equations

- Vorticity equation [Chen PoP 17], derived from quasi-neutrality condition $\boldsymbol{\nabla}\cdot\delta\boldsymbol{J}=0$:

$$\begin{aligned}\mathscr{L}_A(\Phi_s)\equiv & B_0\nabla_\parallel\left(\frac{1}{B_0}\nabla_\perp^2\nabla_\parallel\Phi_s\right)-\boldsymbol{\nabla}_\perp\cdot\left(\frac{\partial_t^2}{v_A^2}\boldsymbol{\nabla}_\perp\Phi_s\right)\\ &+\frac{8\pi}{B_0}(\boldsymbol{b}_0\times\boldsymbol{\kappa})\cdot\boldsymbol{\nabla}_\perp\left[\frac{\boldsymbol{b}_0}{B_0}\cdot(\boldsymbol{\nabla}P_0\times\boldsymbol{\nabla}_\perp\Phi_s)\right]\\ &\cancel{+\frac{4\pi}{cB_0}\left[\boldsymbol{b}_0\times\boldsymbol{\nabla}_\perp(\nabla_\parallel\Phi_s)\right]\cdot\boldsymbol{\nabla}J_{0\parallel}}\\ &=-\frac{8\pi}{cB_0}(\boldsymbol{b}_0\times\boldsymbol{\kappa})\cdot\boldsymbol{\nabla}_\perp\delta P_{\mathrm{comp}}.\end{aligned}\tag{1}$$

- Perturbed pressure equation:

$$\begin{aligned}\mathscr{L}_S(\delta P_{\mathrm{comp}})\equiv & \partial_t^2\delta P_{\mathrm{comp}}-c_S^2B_0\nabla_\parallel\left(\frac{1}{B_0}\nabla_\parallel\delta P_{\mathrm{comp}}\right)\\ &=-\frac{2\Gamma P_0c}{B_0}(\boldsymbol{b}_0\times\boldsymbol{\kappa})\cdot\boldsymbol{\nabla}_\perp\partial_t^2\Phi_s.\end{aligned}\tag{2}$$

- $\Phi_s\rightarrow$ perturbed stream function, $\delta\boldsymbol{\xi}_\perp=\frac{c}{B_0}\boldsymbol{b}\times\boldsymbol{\nabla}\Phi_s$; $\delta P_{comp}=-\Gamma P_0\boldsymbol{\nabla}\cdot\delta\boldsymbol{\xi}$

  $\rightarrow$ compressional component of perturbed pressure.

Model equations

- Equilibrium magnetic field:

$$\boldsymbol{B}_0 = F(\psi)\nabla\varphi + \nabla\psi \times \nabla\varphi.$$

- Boozer coordinates (ψ, θ, ζ): magnetic field line is straightened; JB_0^2 is a flux function.
- Ballooning mode representation [Lu PoP 12]:

$$\begin{aligned} f(r,\theta,\zeta) &= \sum_{m\in\mathbb{Z}} A_n(r) e^{i(n\zeta - m\theta)} \int d\vartheta e^{i(m-nq)\vartheta} \hat{f}_n(r,\vartheta) \\ &= 2\pi A_n(r) \sum_{\ell\in\mathbb{Z}} e^{in\zeta - inq(\theta - 2\pi\ell)} \hat{f}_n(r, \theta - 2\pi\ell). \end{aligned} \tag{3}$$

$$f(r,\theta,\zeta) = e^{in\zeta} f_n(r,\theta) = \sum_m e^{in\zeta - im\theta} f_{n,m}(r),$$

$$f_{n,m}(r) = f_n(r, nq - m) = \int_{-\infty}^{+\infty} d\vartheta e^{-i(nq-m)\vartheta} \hat{f}_n(r,\vartheta),$$

$$\sum_m e^{im\vartheta} = 2\pi \sum_\ell \delta(\vartheta - 2\pi\ell).$$

Model equations

- Mapping relation of ballooning mode representation:

$$\begin{aligned} \partial_\theta &\mapsto \partial_\vartheta - inq, \\ \partial_r &\mapsto inq'(\theta_k - \vartheta), \\ p(\theta) &\mapsto p(\vartheta). \end{aligned}$$

- Coupled SAW-ISW equations in ballooning space:

$$\begin{aligned} &\left[\partial_\vartheta^2 - \frac{\partial_\vartheta^2 \hat{\kappa}_\perp}{\hat{\kappa}_\perp} + \frac{\omega^2 \mathcal{J}^2 B_0^2}{v_A^2} - 8\pi \mathcal{J}^2 \frac{r B_0 P'}{q \hat{\kappa}_\perp \psi'} \left(\kappa_g \frac{\nabla\psi \cdot \hat{\boldsymbol{\kappa}}_\perp}{\hat{\kappa}_\perp |\nabla\psi|} - \kappa_n \frac{r B_0}{q \hat{\kappa}_\perp |\nabla\psi|}\right)\right] g_1(\vartheta) \\ &= -(2\Gamma\beta)^{1/2} \frac{\mathcal{J}^2 B_0^2}{q R_0} \left(\kappa_g \frac{\nabla\psi \cdot \hat{\boldsymbol{\kappa}}_\perp}{\hat{\kappa}_\perp |\nabla\psi|} - \kappa_n \frac{r B_0}{q \hat{\kappa}_\perp |\nabla\psi|}\right) g_2(\vartheta), \\ &\left(\frac{\mathcal{J}^2 B_0^2}{q^2 R_0^2} + \frac{\omega_S^2}{\omega^2} \partial_\vartheta^2\right) g_2(\vartheta) = -(2\Gamma\beta)^{1/2} \frac{\mathcal{J}^2 B_0^2}{q R_0} \left(\kappa_g \frac{\nabla\psi \cdot \hat{\boldsymbol{\kappa}}_\perp}{\hat{\kappa}_\perp |\nabla\psi|} - \kappa_n \frac{r B_0}{q \hat{\kappa}_\perp |\nabla\psi|}\right) g_1(\vartheta), \end{aligned} \tag{4}$$

- $g_1(\vartheta) = \frac{\widehat{\phi}_s(\vartheta)}{(\beta q^2)^{1/2}} \frac{c k_\vartheta}{B_0 R_0}$ with $\widehat{\phi}_s(\vartheta) = \hat{\kappa}_\perp \widehat{\Phi}_s(\vartheta)$, $g_2(\vartheta) = \frac{i\delta \widehat{P}_{comp}(\vartheta)}{(2\Gamma)^{1/2} P_0}$, and

$$\kappa_g = \frac{F(\psi)}{|\nabla\psi|} \frac{\partial_\theta B_0}{\mathcal{J} B_0^2}, \quad \kappa_n = \frac{|\nabla\psi|}{B_0} \left(\partial_\psi B_0 + \frac{4\pi}{B_0} \partial_\psi P_0\right) + \frac{\boldsymbol{\nabla}\psi \cdot \boldsymbol{\nabla}\theta}{|\nabla\psi|} \frac{\partial_\theta B_0}{B_0},$$

$$\hat{\boldsymbol{\kappa}}_\perp = \frac{\boldsymbol{k}_\perp}{k_\theta} = \left[(s\vartheta - s\theta_k) \boldsymbol{\nabla} r + r \boldsymbol{\nabla}\theta - \frac{r}{q} \boldsymbol{\nabla}\zeta\right] (1 + \mathscr{O}(1/nq)).$$

Model equations

- Slow sound approximation [Chu PFB 92], valid for $\omega \gg k_\parallel c_S$:

$$\left[\partial_\vartheta^2 - \frac{\partial_\vartheta^2 \hat{\kappa}_\perp}{\hat{\kappa}_\perp} + \frac{\omega^2 \mathcal{J}^2 B_0^2}{v_A^2} - 8\pi \mathcal{J}^2 \frac{r B_0 P'}{q \hat{\kappa}_\perp \psi'} \left(\kappa_g \frac{\nabla\psi \cdot \hat{\boldsymbol{\kappa}}_\perp}{\hat{\kappa}_\perp |\nabla\psi|} - \kappa_n \frac{r B_0}{q \hat{\kappa}_\perp |\nabla\psi|}\right)\right] g_1 = 2\Gamma\beta \mathcal{J}^2 B_0^2 \left(\kappa_g \frac{\nabla\psi \cdot \hat{\boldsymbol{\kappa}}_\perp}{\hat{\kappa}_\perp |\nabla\psi|} - \kappa_n \frac{r B_0}{q \hat{\kappa}_\perp |\nabla\psi|}\right)^2 g_1. \quad (5)$$

- In the following, the model equations will be written in the following form for simplicity:

$$\frac{d}{d\vartheta}\mathbf{g}(\vartheta) = \mathbf{V}(\omega;\vartheta)\mathbf{g}(\vartheta)$$

- $\mathbf{g} = (g_1, g_1', g_2, g_2')^{\mathrm{T}}$ in full SAW-ISW system, and $\mathbf{g} = (g_1, g_1')^{\mathrm{T}}$ in slow sound approximation.

Outline

- **Background**
- **Theoretical framework**
  - Model equations: ideal MHD equations in ballooning space
  - Solving method: Floquet solutions $\Longrightarrow$ boundary condition
- **Numerical results**
  - Frequency and mode structure of TAE in DTT (slow sound approximation)
  - Effect of triangularity on TAE (slow sound approximation)
  - Finite damping rate and radial singular structure of TAE due to the coupling with acoustic continuum (full SAW-ISW system)
- **Summary and prospect**

Solving method

浙江大学 ZHEJIANG UNIVERSITY

- In the large-$|\vartheta|$ limit, $\mathbf{V}_0(\omega;\vartheta+2\pi)=\mathbf{V}_0(\omega;\vartheta) \Longrightarrow$ Floquet theory can be adopted.

$$\frac{d}{d\vartheta}\boldsymbol{g}(\vartheta)=\mathbf{V}(\omega;\vartheta)\boldsymbol{g}(\vartheta) \xrightarrow{|\vartheta|\to\infty} \frac{d}{d\vartheta}\boldsymbol{g}(\vartheta)=\mathbf{V}_0(\omega;\vartheta)\boldsymbol{g}(\vartheta)$$

- According to Floquet theory, it must have the solutions in the form of

$$\mathbf{x}_i(\omega;\vartheta)=\mathbf{P}_i(\vartheta)e^{i\nu_i\vartheta}.$$

- For each ω in the range of interest, we take the corresponding Floquet solutions $\mathbf{x}_i(\omega;\vartheta)$ as the boundary condition.

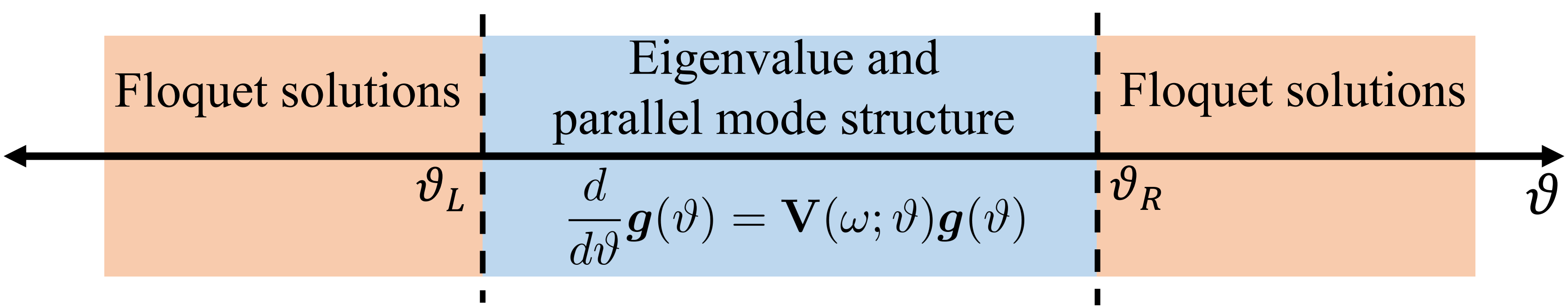

Outline

- **Background**
- **Theoretical framework**
  - Model equations: ideal MHD equations in ballooning space
  - Solving method: Floquet solutions $\Longrightarrow$ boundary condition
- **Numerical results**
  - Frequency and mode structure of TAE in DTT (slow sound approximation)
  - Effect of triangularity on TAE (slow sound approximation)
  - Finite damping rate and radial singular structure of TAE due to the coupling with acoustic continuum (full SAW-ISW system)
- **Summary and prospect**

DTT: **D**ivertor **T**okamak **T**est facility, a D-shaped superconducting device, which is being built at the ENEA Research Center in Frascati, Italy.

Parameter	DTT
Minor radius	6.5×10^{-1} m
Aspect ratio	3.3
Toroidal field	6.0 T
Plasma current	5.5×10^{6} A
Additional power	4.5×10^{7} W

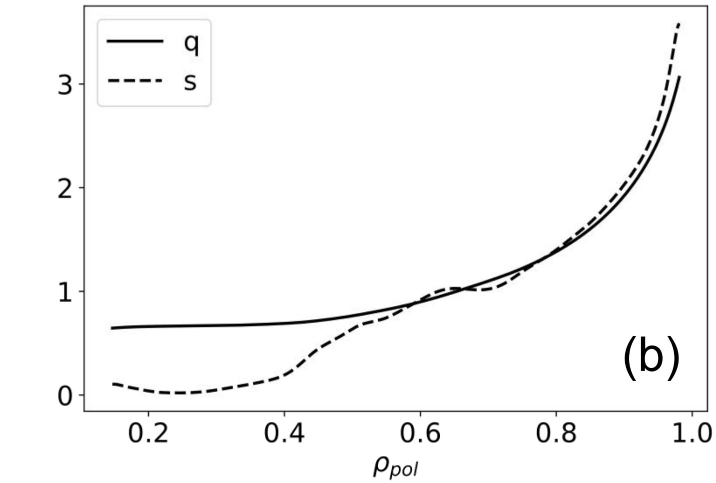

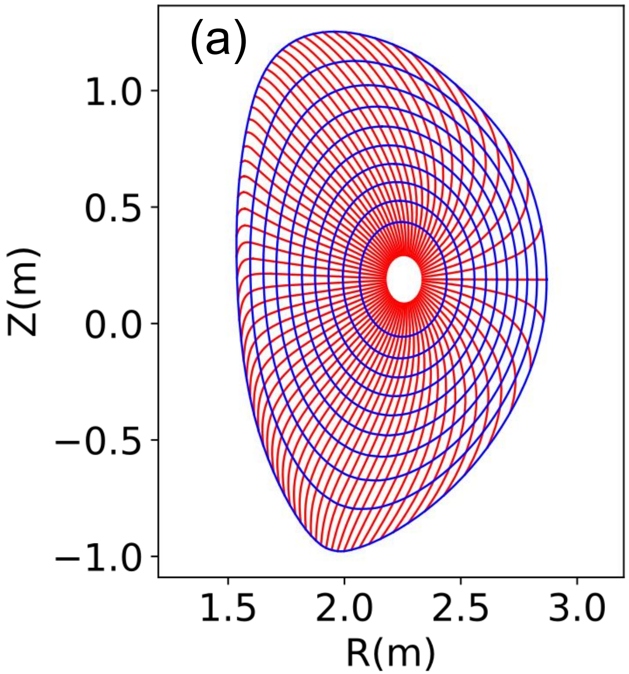

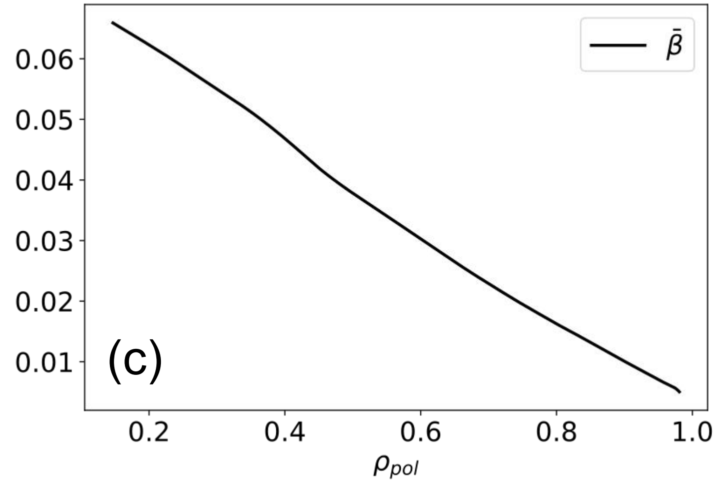

Floquet solutions ($\rho_{pol} = 0.702$)

$$\Omega = \omega R_0/\bar{v}_{A0}$$

$\nu = |nq - m|$ gives the frequencies of the local continuous spectrum.

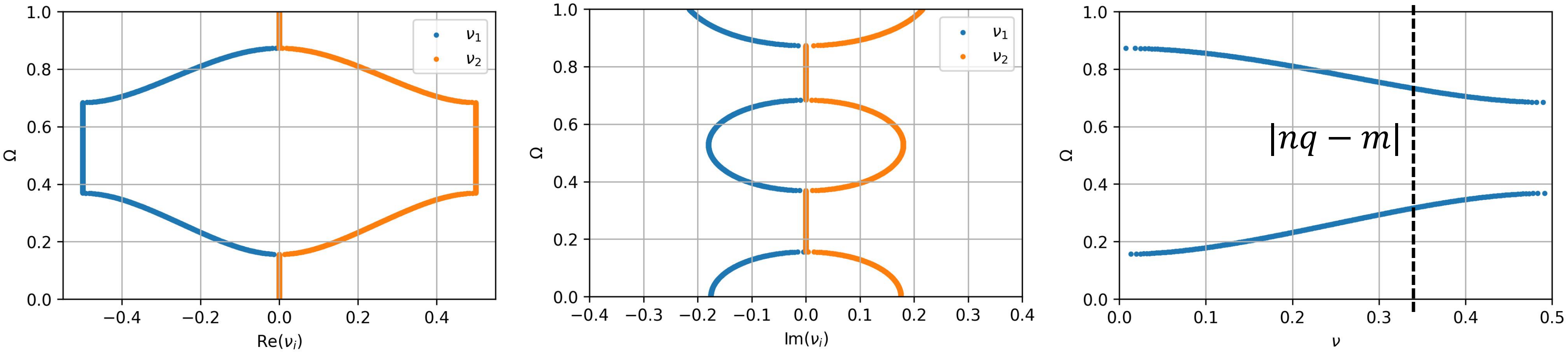

Boundary condition can be chosen easily from Floquet solutions $\mathbf{x}_i(\vartheta) = \mathbf{P}_i(\vartheta)e^{i\nu_i\vartheta}$.

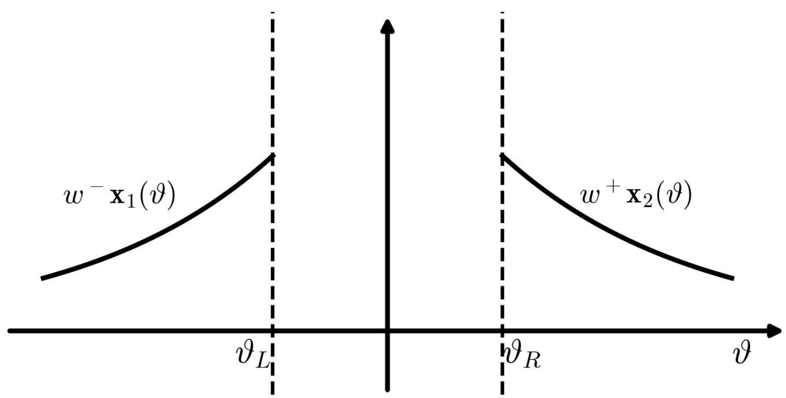

Solutions of $(g_1, g_1')^T$ on the left and right matching at zero leads to

$$\mathbf{M}(\omega)\mathbf{w} = 0,$$

where $\mathbf{w} = (w^-, w^+)^T$. $\det\left(\mathbf{M}(\omega)\right) = 0$ gives the dispersion relation.

TAE frequency and mode structure in DTT

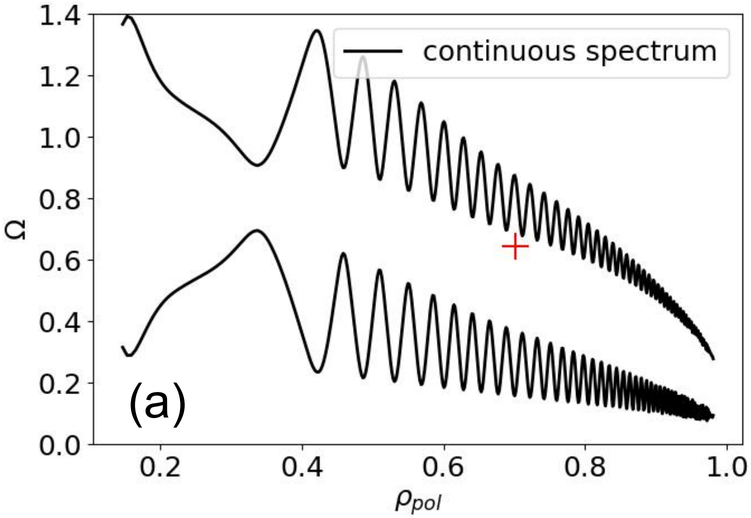

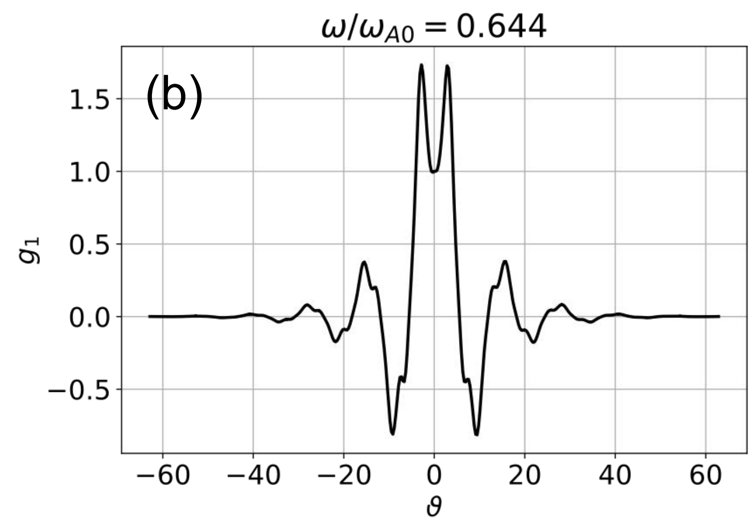

$$f(r,\theta,\zeta) = \sum_{m\in\mathbb{Z}} A_n(r) e^{i(n\zeta - m\theta)} \int d\vartheta e^{i(m-nq)\vartheta} \hat{f}_n(\vartheta)$$
$$= 2\pi A_n(r) \sum_{\ell\in\mathbb{Z}} e^{in\zeta - inq(\theta - 2\pi\ell)} \hat{f}_n(\theta - 2\pi\ell).$$

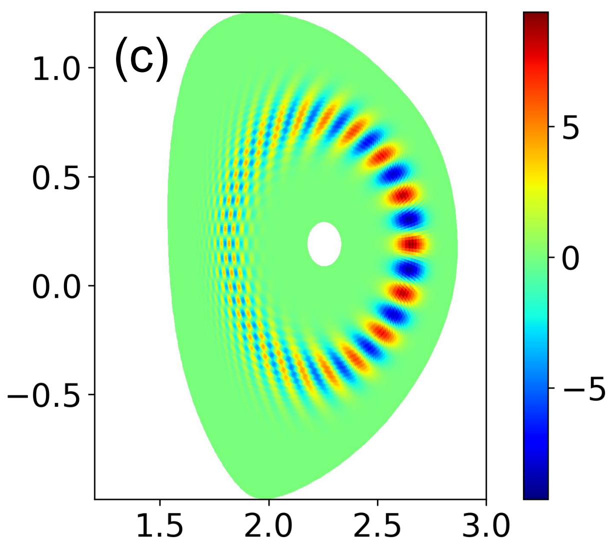

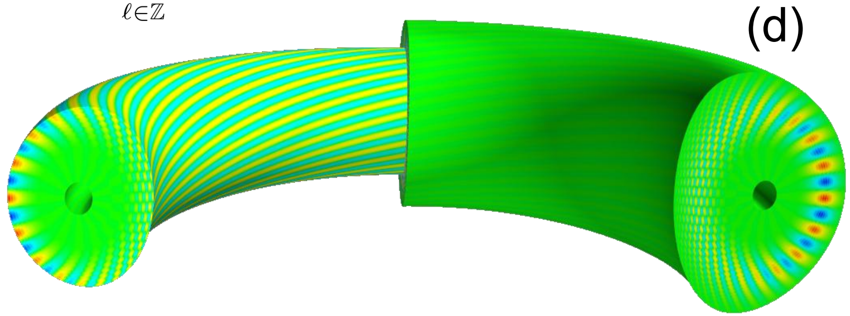

(a) Continuous spectrum (n=20) and location of TAE. (b) Parallel mode structure of TAE at $\rho_{pol} = 0.702$. (c) 2D (d) 3D mode structure (n=20) obtained with an artificial radial envelop.

Outline

- **Background**
- **Theoretical framework**
  - Model equations: ideal MHD equations in ballooning space
  - Solving method: Floquet solutions $\Longrightarrow$ boundary condition
- **Numerical results**
  - Frequency and mode structure of TAE in DTT (slow sound approximation)
  - Effect of triangularity on TAE (slow sound approximation)
  - Finite damping rate and radial singular structure of TAE due to the coupling with acoustic continuum (full SAW-ISW system)
- **Summary and prospect**

Effect of magnetic geometry

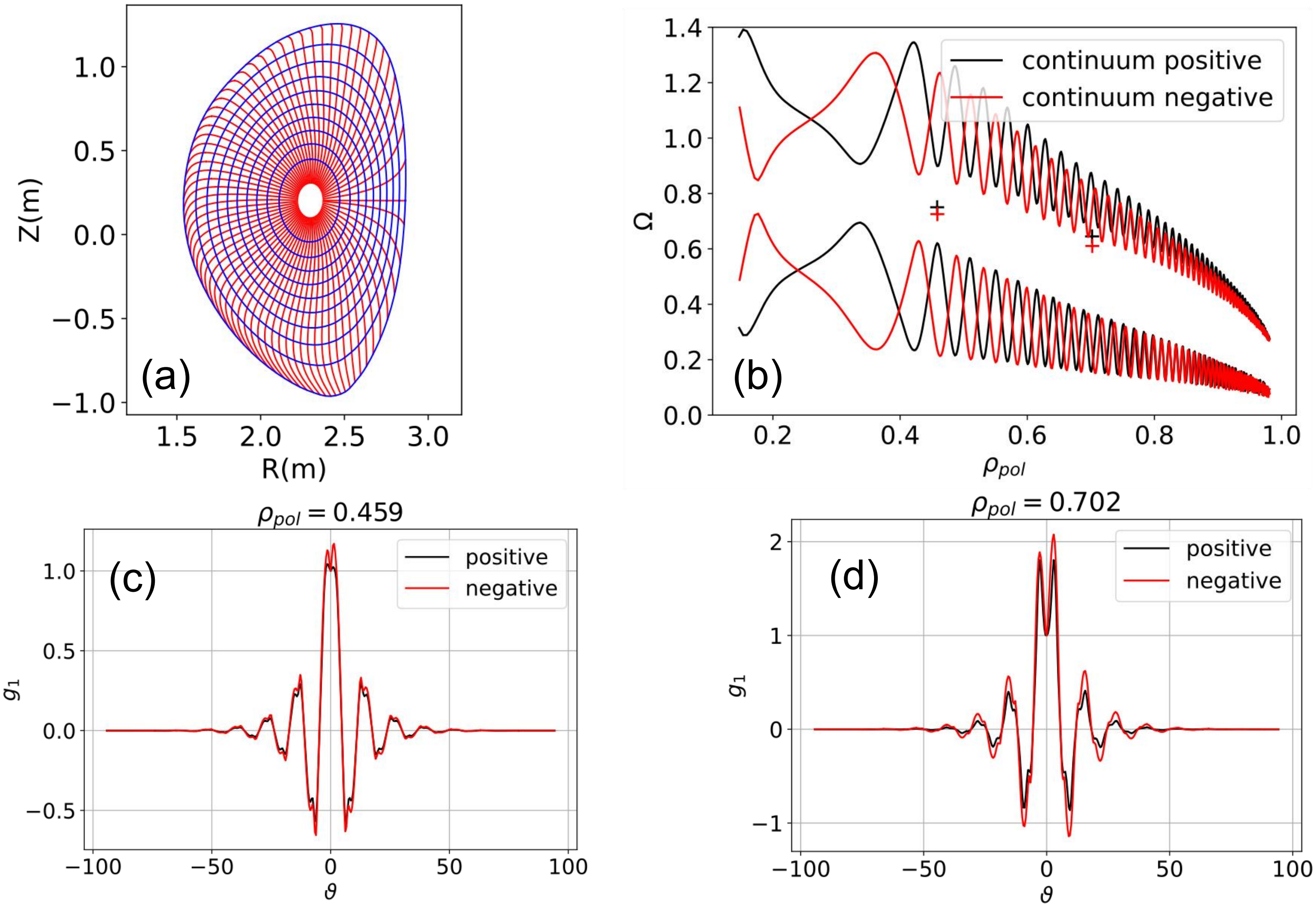

(a) Contour lines of ψ and isolines of θ for negative triangularity equilibrium. (b) Continuous spectrum for the two equilibria. (c) Parallel mode structure at $\rho_{pol} = 0.459$ for the two equilibria. (d) Parallel mode structure at $\rho_{pol} = 0.702$ for the two equilibria.

Effect of triangularity

Local Miller equilibrium [Miller PoP 99]

Flux surface:

$$R = R_0 + r\cos(\theta + \delta \sin\theta),$$
$$Z = \kappa r \sin\theta.$$

Magnetic field:

$$B_t = \frac{F}{R}, \quad B_p = \frac{\psi'}{R}|\nabla r|.$$

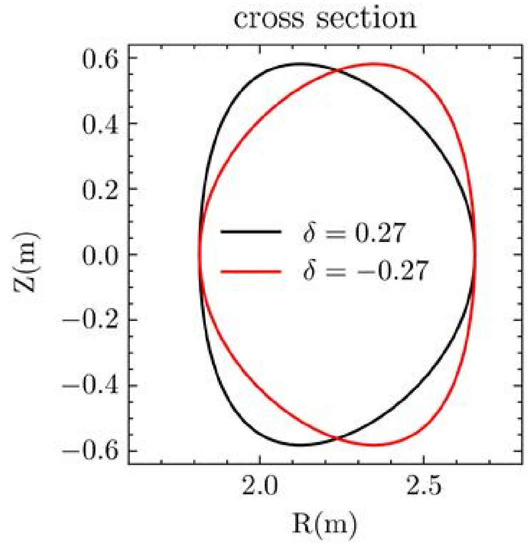

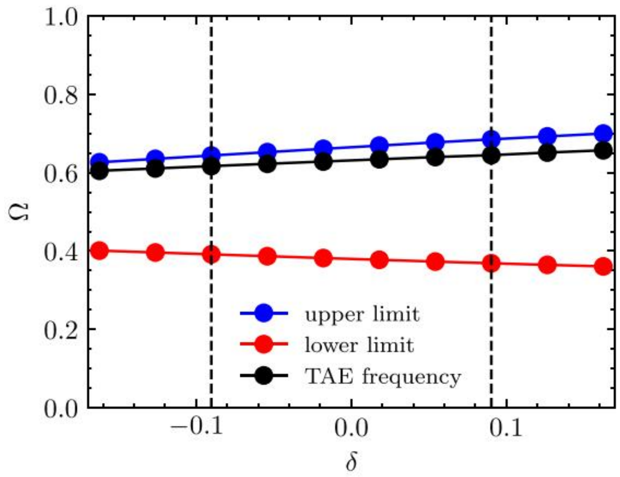

$$\left[\partial_\vartheta^2 - \frac{\partial_\vartheta^2 \hat{\kappa}_\perp}{\hat{\kappa}_\perp} + \frac{\omega^2 \mathcal{J}^2 B_0^2}{v_A^2} - 8\pi \mathcal{J}^2 \frac{r B_0 P'}{q \hat{\kappa}_\perp \psi'} \left(\kappa_g \frac{\nabla\psi \cdot \hat{\boldsymbol{\kappa}}_\perp}{\hat{\kappa}_\perp |\nabla\psi|} - \kappa_n \frac{r B_0}{q \hat{\kappa}_\perp |\nabla\psi|}\right)\right] g_1$$
$$= 2\Gamma\beta \mathcal{J}^2 B_0^2 \left(\kappa_g \frac{\nabla\psi \cdot \hat{\boldsymbol{\kappa}}_\perp}{\hat{\kappa}_\perp |\nabla\psi|} - \kappa_n \frac{r B_0}{q \hat{\kappa}_\perp |\nabla\psi|}\right)^2 g_1.$$

1. The value of δ is generally small near the core region.
2. The dependence of the Jacobi on δ is weak.
3. TAE is dominated by the $\cos\theta$-type variation of the magnetic field.

$$\mathcal{J}_0 = (\nabla\psi \times \nabla\theta \cdot \nabla\phi)^{-1} = \frac{1}{\psi'} \det\left[\frac{\partial(R, Z)}{\partial(r, \theta)}\right] R$$
$$= \frac{r}{\psi'} \left\{R_0' \kappa \cos\theta + \kappa \cos(\delta \sin\theta) + \sin(\theta + \delta \sin\theta) \sin\theta \left[\cos\theta(\delta\kappa + r\delta\kappa' - r\delta'\kappa) + r\kappa'\right]\right\}$$
$$\left[R_0 + r\cos(\theta + \delta\sin\theta)\right].$$

Outline

- **Background**
- **Theoretical framework**
  - Model equations: ideal MHD equations in ballooning space
  - Solving method: Floquet solutions $\Longrightarrow$ boundary condition
- **Numerical results**
  - Frequency and mode structure of TAE in DTT (slow sound approximation)
  - Effect of triangularity on TAE (slow sound approximation)
  - Finite damping rate and radial singular structure of TAE due to the coupling with acoustic continuum (full SAW-ISW system)
- **Summary and prospect**

Floquet solutions

Outgoing wave: $\frac{\partial \omega}{\partial \nu} < 0$ on the left and $\frac{\partial \omega}{\partial \nu} > 0$ on the right

$\nu = |nq - m|$ gives the frequencies of the local continuous spectrum.

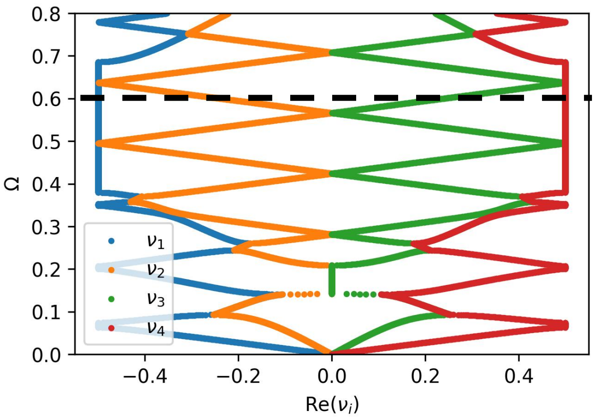

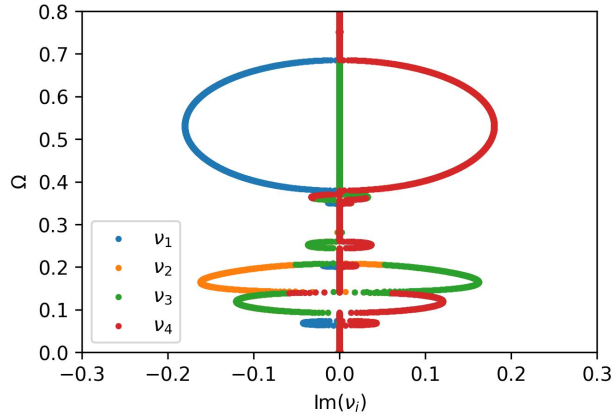

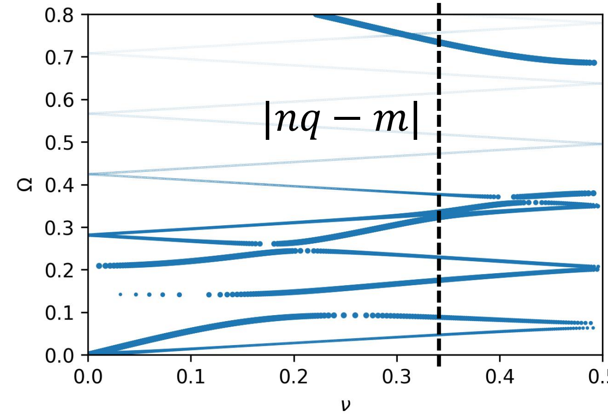

$$\mathcal{A} = \frac{\int_0^{2\pi} |g_1(\nu_i, \vartheta)|^2 \, d\vartheta}{\int_0^{2\pi} \left[|g_1(\nu_i, \vartheta)|^2 + |g_2(\nu_i, \vartheta)|^2 \right] d\vartheta}$$

Boundary condition can be chosen easily from Floquet solutions $\mathbf{x}_i(\vartheta) = \mathbf{P}_i(\vartheta) e^{i\nu_i \vartheta}$.

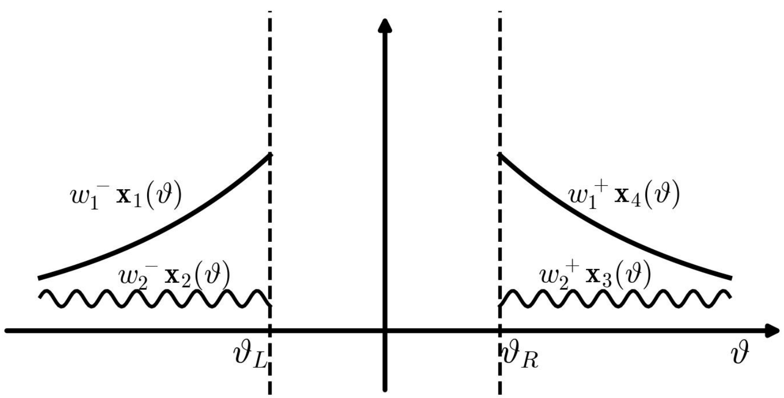

Solutions of $(g_1, g_1', g_2, g_2')^T$ on the left and right matching at zero leads to

$$\mathbf{M}(\omega)\mathbf{w} = 0,$$

$\mathbf{w} = (w_1^-, w_2^-, w_1^+, w_2^+)^T$. $\det(\mathbf{M}(\omega)) = 0$ gives the dispersion function $D(\omega)$.

TAE frequency & parallel mode structure

- Considering $\Omega_i \ll \Omega_r$, Ω_i can be solved perturbatively: $\Omega_i = -\frac{D_i}{\partial D_r/\partial \Omega_r}$.
- In the TAE gap ($[\Omega_L, \Omega_U]$), find Ω_r that minimizes $|D(\Omega_r)|$.

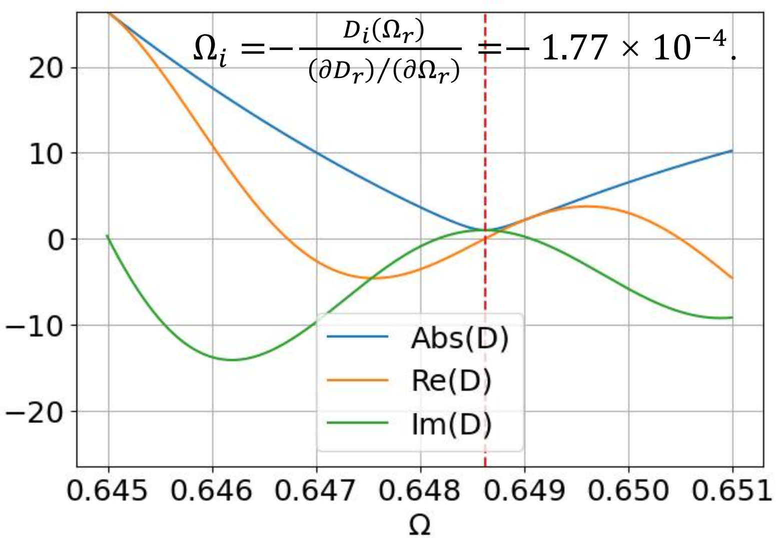

$\overline{\beta} = 2.3\%$

$\Omega = 0.645$

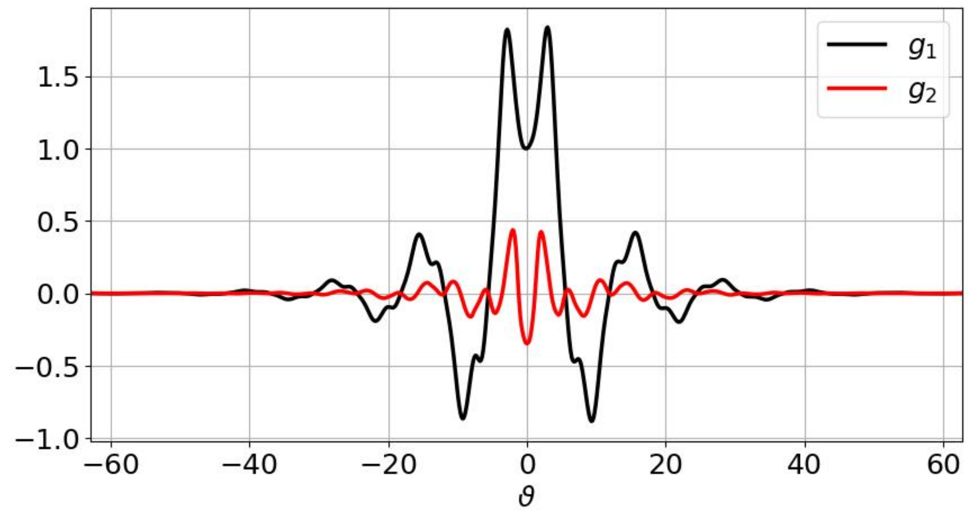

$\Omega = 0.649 - 1.77 \times 10^{-4} i$

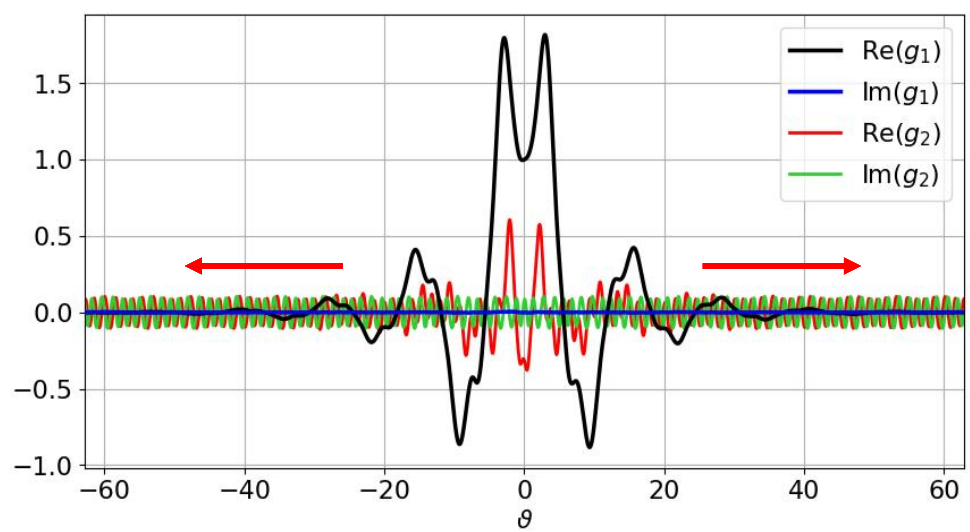

Mode structure in real space

- m-th poloidal harmonic: $f(nq-m)=\int_{-\vartheta_b}^{\vartheta_b} d\vartheta e^{-i(nq-m)\vartheta}\hat{f}(\vartheta)$.
- By truncating a series of gradually increasing window sizes $[-\vartheta_b, \vartheta_b]$ of the parallel mode structure and transforming them into real space, we may "simulate" the "time evolution" of the mode structure in real space.

"time evolution" of the mode structure in real space

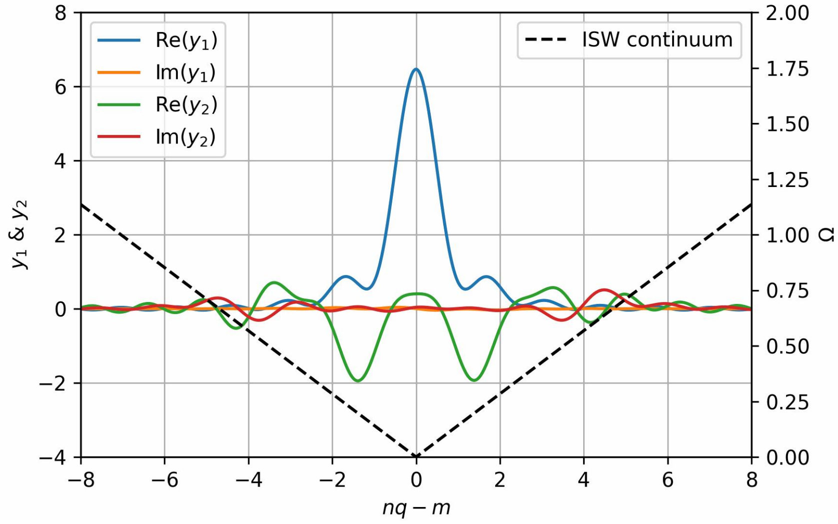

Eigenmode solution with radial oscillation phase mixed away

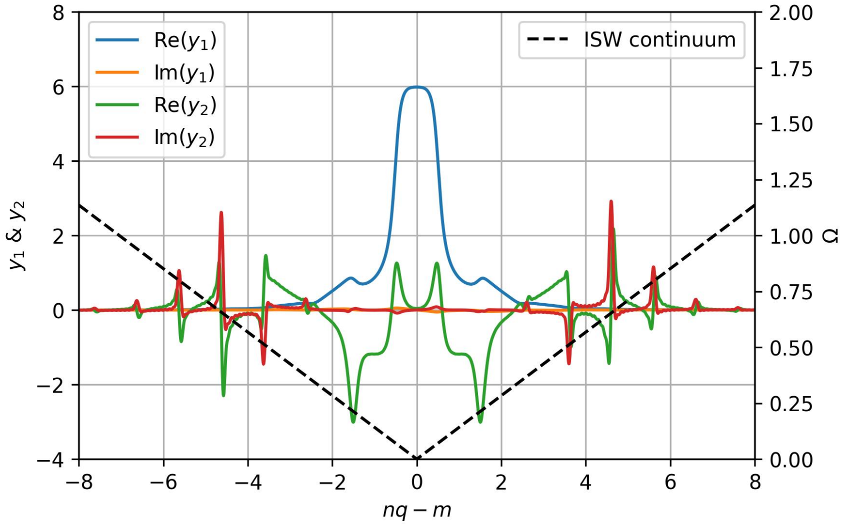

- The generation of radial singular structure at the intersection of the mode frequency and the ISW continuum is observed.

Outline

- **Background**
- **Theoretical framework**
  - Model equations: ideal MHD equations in ballooning space
  - Solving method: Floquet solutions $\Longrightarrow$ boundary condition
- **Numerical results**
  - Frequency and mode structure of TAE in DTT (slow sound approximation)
  - Effect of triangularity on TAE (slow sound approximation)
  - Finite damping rate and radial singular structure of TAE due to the coupling with acoustic continuum (full SAW-ISW system)
- **Summary and prospect**

Summary

浙江大學 ZHEJIANG UNIVERSITY

- We developed an eigenvalue code based on FALCON to calculate the frequency and parallel mode structure of AEs.
- Characteristics: ideal MHD; ballooning mode representation; general geometry.
- Slow sound approximation ⇒ focusing on TAE frequency range.
- Applications: frequency and parallel mode structure of TAE in DTT equilibrium; effect of triangularity.
- Novel result in the full SAW-ISW system: finite damping rate and radial singular structure of TAE due to the coupling with acoustic continuum.

Prospect

- Extend to kinetic model to investigate various kinetic effects (ongoing work).
- Solve the global eigenvalue problem to get the radial envelope self-consistently.

Thanks for your attention!

Variational principle

$$\left[\partial_\vartheta^2 - \frac{\partial_\vartheta^2 \hat{\kappa}_\perp}{\hat{\kappa}_\perp} + \frac{\omega^2 \mathcal{J}^2 B_0^2}{v_A^2} - 8\pi \mathcal{J}^2 \frac{r B_0 P'}{q \hat{\kappa}_\perp \psi'} \left(\kappa_g \frac{\nabla\psi \cdot \hat{\boldsymbol{\kappa}}_\perp}{\hat{\kappa}_\perp |\nabla\psi|} - \kappa_n \frac{r B_0}{q \hat{\kappa}_\perp |\nabla\psi|}\right)\right] g_1(\vartheta)$$

$$= -(2\Gamma\beta)^{1/2} \frac{\mathcal{J}^2 B_0^2}{q R_0} \left(\kappa_g \frac{\nabla\psi \cdot \hat{\boldsymbol{\kappa}}_\perp}{\hat{\kappa}_\perp |\nabla\psi|} - \kappa_n \frac{r B_0}{q \hat{\kappa}_\perp |\nabla\psi|}\right) g_2(\vartheta), \qquad \text{(a)}$$

$$\left(\frac{\mathcal{J}^2 B_0^2}{q^2 R_0^2} + \frac{\omega_S^2}{\omega^2} \partial_\vartheta^2\right) g_2(\vartheta) = -(2\Gamma\beta)^{1/2} \frac{\mathcal{J}^2 B_0^2}{q R_0} \left(\kappa_g \frac{\nabla\psi \cdot \hat{\boldsymbol{\kappa}}_\perp}{\hat{\kappa}_\perp |\nabla\psi|} - \kappa_n \frac{r B_0}{q \hat{\kappa}_\perp |\nabla\psi|}\right) g_1(\vartheta), \qquad \text{(b)}$$

$$\int_{-\infty}^{\infty} \left\{ g_1^* \cdot (\mathrm{a}) - g_1 \cdot (\mathrm{a})^* + \left[g_2^* \cdot (\mathrm{b}) - g_2 \cdot (\mathrm{b})^*\right] \right\} d\vartheta,$$

$$4i\omega_r\omega_i \int_{-\infty}^{\infty} \frac{\mathcal{J}^2 B_0^2}{v_A^2} |g_1|^2 d\vartheta = -\left(g_1^* \partial_\vartheta g_1 - g_1 \partial_\vartheta g_1^*\right)\Big|_{-\infty}^{\infty} - \frac{\omega_S^2}{\omega_r^2}\left(g_2^* \partial_\vartheta g_2 - g_2 \partial_\vartheta g_2^*\right)\Big|_{-\infty}^{\infty}.$$

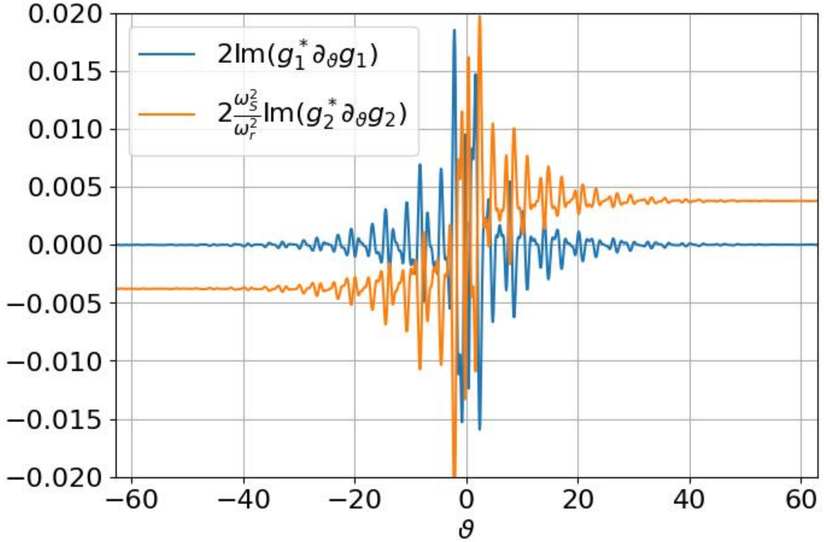

- Variational principle: $\Omega_i = -1.95 \times 10^{-4}$ (perturbation method: $\Omega_i = -1.77 \times 10^{-4}$)
- Solution of Ω in the complex space is consistent with these two approximate methods.